Physics Letters B ••• (••••) •••–•••

Contents lists available at ScienceDirect

Physics Letters B

www.elsevier.com/locate/physletb

Re-estimation of ^{180}Ta nucleosynthesis in light of newly constrained reaction rates

K.L. Malatji [a,b,*], M. Wiedeking [a], S. Goriely [c], C.P. Brits [a,b], B.V. Kheswa [a,d], F.L. Bello Garrote [e], D.L. Bleuel [f], F. Giacoppo [e,g,h], A. Görgen [e], M. Guttormsen [e], K. Hadynska-Klek [e], T.W. Hagen [e], V.W. Ingeberg [e], M. Klintefjord [e], A.C. Larsen [e], P. Papka [a,b], T. Renstrøm [e], E. Sahin [e], S. Siem [e], L. Siess [c], G.M. Tveten [e], F. Zeiser [e]

[a] iThemba LABS, P.O. Box 722, 7129 Somerset West, South Africa
[b] Physics Department, University of Stellenbosch, Matieland, 7602, South Africa [1]
[c] Institut d'Astronomie et d'Astrophysique, Université Libre de Bruxelles, CP 226, B-1050 Brussels, Belgium
[d] Department of Applied Physics and Engineering Mathematics, University of Johannesburg, Johannesburg, 2028, South Africa
[e] Department of Physics, University of Oslo, N-0316 Oslo, Norway
[f] Lawrence Livermore National Laboratory, Livermore, CA 94551, USA
[g] Helmholtz Institute Mainz, 55099 Mainz, Germany
[h] GSI Helmholtzzentrum für Schwerionenforschung GmbH, 64291 Darmstadt, Germany

ARTICLE INFO

Article history:
Received 10 January 2019
Received in revised form 25 February 2019
Accepted 6 March 2019
Available online xxxx
Editor: W. Haxton

Keywords:
Nuclear level density
γ-ray strength function
(n,γ) cross sections
Maxwellian-averaged cross sections
Nucleosynthesis

ABSTRACT

Recent measurements of the nuclear level densities and γ-ray strength functions below the neutron thresholds in ^{180,181,182}Ta are used as input in the nuclear reaction code TALYS. These experimental average quantities are utilized in the calculations of the ^{179,180,181}Ta radiative neutron capture cross sections. From the latter, astrophysical Maxwellian-averaged (n,γ) cross sections (MACS) and reaction rates are extracted, which in turn are used in large astrophysical network calculations to probe the production mechanism of ^{180}Ta. These calculations are performed for two scenarios, the *s*-process production of ^{180,181}Ta in Asymptotic Giant Branch (AGB) stars and the *p*-process nucleosynthesis of ^{180}Ta^m in Type-II supernovae. Based on the results from this work, the *s*-process in stellar evolution is considered negligible in the production of ^{180}Ta^m whereas ^{181}Ta is partially produced by AGB stars. The new measurements strongly constrain the production and destruction rates of ^{180}Ta^m at *p*-process temperatures and confirm significant production of nature's rarest stable isotope ^{180}Ta^m by the *p*-process.

1. Introduction

A small number of naturally occurring neutron-deficient nuclides with $Z \geq 34$, referred to as *p*-nuclei, cannot be produced by neutron-capture processes [1]. Instead, these stable nuclides with $74 \leq A \leq 196$ are thought to be produced by the photodisintegration (*p*-process) of slow-neutron capture (*s*-process) and rapid-neutron capture (*r*-process) seed nuclei [1]. However, for ^{138}La and ^{180}Ta, for instance, the *p*-process is not sufficient to explain their observed solar abundances and additional processes are invoked. While the situation for ^{180}Ta is not clear, it was shown that for ^{138}La the photodisintegration of seed nuclei is not efficient enough but that neutrino (ν) captures during the *p*-process in Type-II supernovae may be responsible for its galactic enrichment [2–4].

A peculiar feature of ^{180}Ta is that it is the rarest isotope found in the solar system, with an isotopic abundance of only 0.012% existing in a $J^\pi = 9^-$ isomeric state at an excitation energy $E_x =$ 77 keV with a half-life of $\approx 10^{15}$ yr.

The ^{180}Ta production mechanism invokes controversy since calculations show that several nucleosynthesis processes, sometimes exclusively, can reproduce the observed ^{180}Ta abundance [5], making it a particularly interesting case to study. The *s*-, *r*- and *p*-processes in high-density, high-temperature environments, have all been proposed to explain the synthesis of ^{180}Ta. It has been theoretically shown that ^{180}Ta galactic enrichment could be ex-

* Corresponding author at: iThemba LABS, P.O. Box 722, 7129 Somerset West, South Africa.
E-mail addresses: klmalatji@tlabs.ac.za (K.L. Malatji), wiedeking@tlabs.ac.za (M. Wiedeking).
[1] Also at Department of Applied Physics and Engineering Mathematics, University of Johannesburg, Johannesburg, 2028, South Africa.

https://doi.org/10.1016/j.physletb.2019.03.013

clusively explained by the p-process [2,6,7]. In explosive environments, neutrino captures and scattering reactions, which include ^{180}Hf$(\nu_e, e)^{180}$Ta and ^{181}Ta$(\nu, \nu' n)^{180}$Ta, have also been proposed to significantly contribute to its synthesis [2,5,8–10]. Additionally, the s-process has been invoked to explain the production of ^{180}Ta, mostly via branching in ^{179}Hf through the reaction ^{179}Hf$(\beta^-)^{179}$Ta$(n,\gamma)^{180}$Ta and/or ^{179}Hf$(n,\gamma)^{180}$Hf$^m(\beta^-)^{180}$Ta [11–13].

Since the astrophysical sites for the nucleosynthesis of ^{180}Ta remain unknown, a combination of the above processes is undeniably possible. However, the significance of individual processes cannot be clearly determined, as a result of the uncertainties on the reaction rates for ^{180}Ta due to the unavailability of experimental data, e.g. the radiative neutron capture rates of ^{179,180}Ta isotopes or other nuclear ingredients needed to constrain these rates, such as the nuclear level density (NLD) and γ-ray strength function (γSF) [3]. No NLD and γSF data existed below the neutron separation energy (S_n) for ^{180}Ta, while for ^{181}Ta no data were available for $E_x < 5.8$ MeV until very recently when comprehensive measurements were published for ^{180,181,182}Ta [14,15]. The NLD is described as the average number of nuclear energy levels as a function of excitation energy E_x [16,17], while the γSF gives a measure of the average transition probability for an electromagnetic de-excitation of the nucleus [18]. In the absence of direct cross section measurements, both properties are critical for constraining the radiative neutron capture cross section within the Hauser-Feshbach formalism [19] which is implemented in the nuclear reaction code TALYS [20].

In this letter, the recently measured NLDs and γSFs in ^{180,181,182}Ta [14] are used to determine the ^{179,180,181}Ta(n,γ) cross sections of astrophysical interest. From these, the Maxwellian-averaged cross sections (MACS) are obtained and used in stellar evolution calculations to investigate the role of the s-process in the nucleosynthesis of ^{180,181}Ta. The p-process nucleosynthesis for ^{180}Ta is studied on the basis of the Type-II supernova (SNII) model.

2. Experiments and analysis

In this work, the results of experimental NLDs and γSFs for ^{180,181,182}Ta [14] are being used, and only a brief summary is provided on the measurements of these quantities. ^{3}He and deuteron beams impinge on a natural self-supporting ^{181}Ta metallic foil of 0.8 mg/cm^2 thickness. The reactions with deuteron beams are with i) 12.5 MeV for ^{181}Ta(d, pγ)^{182}Ta and ^{181}Ta(d, d$'\gamma$)^{181}Ta, and with ii) 15 MeV for ^{181}Ta(d, tγ)^{180}Ta and ^{181}Ta(d, d$'\gamma$)^{181}Ta. 34 MeV ^{3}He beams were utilized for ^{181}Ta(^{3}He, ^{3}He$'\gamma$)^{181}Ta and ^{181}Ta(^{3}He, $\alpha\gamma$)^{180}Ta. The light-charged ejectiles in coincidence with γ-rays were detected with the array of 64 $\Delta E - E$ silicon particle telescopes SiRi [21]. The γ-rays were recorded using the high-efficiency multi-detector NaI(Tl) array CACTUS [22]. The NLDs and γSFs were measured for each of the six distinct reactions which populated excited states in ^{180,181,182}Ta.

The measured particle energies in SiRi were converted to E_x of the residual ^{180,181,182}Ta nuclei from reaction kinematics, Q-values and energy losses. The γ-rays were measured in coincidence with CACTUS. The respective E_x versus γ-ray energy (E_γ) matrices are extracted from the particle-γ coincidence events. The Oslo Method [23] is applied to the matrices to extract simultaneously the NLDs and the γSFs, through several iterative methods. The main steps of the Oslo Method include: 1) unfolding the continuum γ-ray spectrum based on the known detector multiple response functions [24] 2) extraction of primary γ-rays from the unfolded γ-ray spectra using the iterative procedure called the first generation method [24] 3) simultaneous extraction of the NLD and the γ-ray transmission coefficients from the primary γ-ray matrix, and 4) the normalization of the NLD and the γ-ray transmission coefficient using the average s-wave neutron resonance data [23,25]. Detailed discussions of the Oslo Method are found in refs. [22–25]. The total NLD at the neutron separation energy, $\rho(S_n)$, was extracted from measured s-wave spacing using three different models, the Back-shifted Fermi-Gas (BSFG) [26], Constant Temperature+Fermi Gas (CT+FG) [20], and Hartree-Fock-Bogoliubov plus Combinatorial (HFB) [27] models. The range of results from these models and their normalizations provide the upper and lower limits in the NLDs and γSFs.

3. (n,γ) cross sections

The experimental NLDs and γSFs from each reaction, taking into account their uncertainties, are now used as input parameters into the TALYS [20] reaction code (version 1.9). The ^{181}Ta$(n,\gamma)^{182}$Ta, ^{180}Ta$^{gs,m}(n,\gamma)^{181}$Ta, and ^{179}Ta$(n,\gamma)^{180}$Ta^{gs,m} cross sections, $\sigma(E_n)$, as a function of incident neutron energies have been calculated. The calculations are based on the Hauser-Feshbach statistical emission model [19] which assumes that the capture reactions occur by means of a compound nuclear system that reaches a statistical equilibrium. The key ingredients to the calculation of (n,γ) cross sections are nuclear structure properties *i.e.* mass, deformation, low-lying level scheme, E_x, J^π, NLDs, γSFs and optical model potentials. The neutron capture reaction cross section $\sigma^\mu_{n,\gamma}(E_n)$, as simplified from Eq. (1) of Ref. [28] is given by

$$\sigma^\mu_{n,\gamma}(E_n) \approx \frac{\pi\lambda\!\!\!^{-2}}{(2J^\mu_I+1)(2J_n+1)} \sum_{J^\pi} (2J+1) T^\mu_\gamma(E, J^\pi). \qquad (1)$$

The neutron transmission coefficient, $T^\mu_n(E, J^\pi)$, is significantly larger than the γ-ray transmission coefficient, $T^\mu_\gamma(E, J^\pi)$, above S_n, and depends on the total angular momentum J, parity π, and energy E_x of the compound system. The target and projectile spins are given by subscripts I and n. The relative wave number $\pi\lambda\!\!\!^{-2} = 0.6566/[m \cdot E^\mu(\text{MeV})]$ barn, where m and E^μ are the reduced mass of the $I^\mu + n$ system and the center-of-mass energy at a level μ, respectively [28]. The γ-ray transmission coefficient, $T^\mu_\gamma(E, J^\pi)$, in Eq. (1) for the decay of the compound nuclear state J^π into any combination of final accessible states is given by the sum of $T^\mu_{XL}(E_\gamma)$ over discrete states μ plus the integral of $T_{XL}(E_\gamma)$ over the nuclear level density $\rho(E_x - E_\gamma)$ in the continuum, for a given multipolarity XL.

The global neutron optical model potential of Ref. [20,29] was used for all nuclei under discussion, as well as the Hofmann-Richert-Tepel-Weidenmüller (HRTW) model [30] for width fluctuation corrections in the compound nucleus calculation. Shown in Fig. 1, are the resulting ^{181}Ta$(n,\gamma)^{182}$Ta, ^{180}Ta$^m(n,\gamma)^{181}$Ta and ^{179}Ta$(n,\gamma)^{180}$Ta^m cross sections. The newly obtained experimental ^{181}Ta$(n,\gamma)^{182}$Ta cross sections, using the BSFG, CT+FG (1 & 2) and HFB normalizations in Fig. 1 (a) show good agreement with each other and with previous Time-of-Flight (ToF) [31,32] and activation [33] measurements.

The experimental ^{180}Ta$^m(n,\gamma)$ cross sections from Ref. [34] are also shown for comparison and agree well with the present cross sections (Fig. 1 (b)). While no comparative experimental data exist, the ^{179}Ta$(n,\gamma)^{180}$Ta^m cross sections (Fig. 1 (c)) are in good agreement with those predicted using microscopic NLD models [35]. The agreement between our results and direct measurements validates that experimental NLDs and γSFs can be used to successfully obtain (n,γ) cross sections and has reliably been used over different mass regions [36–38]. This brings further evidence that

Please cite this article in press as: K.L. Malatji et al., Re-estimation of ^{180}Ta nucleosynthesis in light of newly constrained reaction rates, Phys. Lett. B (2019), https://doi.org/10.1016/j.physletb.2019.03.013

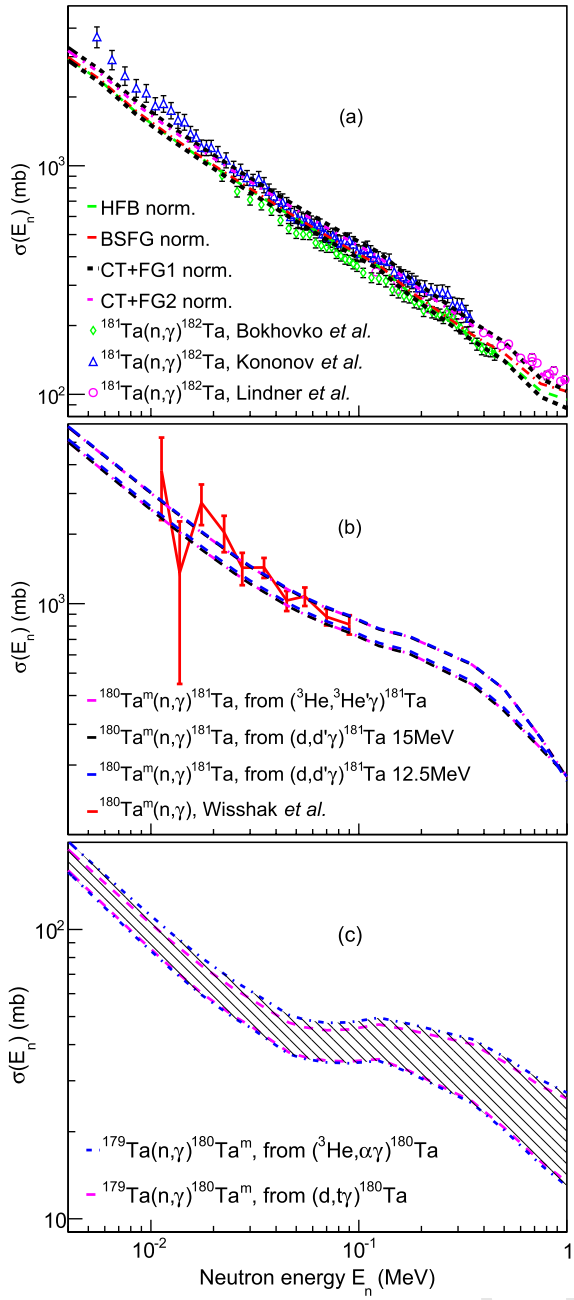

Fig. 1. The ^{179,180,181}Ta(n,γ) cross sections (bands) extracted from the experimental NLDs and γSFs. The ^{181}Ta$(n,\gamma)^{182}$Ta cross sections determined using the BSFG, CT+FG (1 & 2) and HFB models and their normalizations [14] are compared to previous ToF [31,32] and activation [33] measurements (a), and the ^{180}Ta$^{m}(n,\gamma)$ cross section to ToF measurements [34] (b).

this technique can be used when no direct measurements of cross sections are possible [4,39,40]. The (n,γ) cross sections from the experimental NLDs and γSFs obtained using the different reaction channels, are consistent with each other. This is indicative of the robustness of the Oslo Method but also that the results are independent of beam type and beam energies.

In hot stellar environments, the target nucleus is not confined to its ground state but exists in a distribution of thermally excited states μ. At high temperatures T, the relative thermal velocities v_T and excitation energies E_x^μ of nuclei obey a Maxwell-Boltzmann distribution and the thermonuclear reaction rate for neutron induced reactions, in units of cm^3 mol^{-1} s^{-1}, is given by [28]

Table 1
The Maxwellian-averaged (n,γ) cross sections of ^{179,180,181}Ta. The available KADoNiS MACS [41] at *s*-process temperatures are also provided.

Reaction	$\langle E\rangle$ (keV)	Present exp. (mb)	KADoNiS [41] (mb)
^{179}Ta$(n,\gamma)^{180}$Ta^{tot}	30	2006.0 ± 497.0	1334.0 ± 422.0[a]
	215	707.0 ± 233.0	
^{179}Ta$(n,\gamma)^{180}$Ta^{m}	30	56.0 ± 5.0	
	215	34.0 ± 8.0	
^{179}Ta$(n,\gamma)^{180}$Ta^{gs}	30	1950.0 ± 492.0	
	215	679.0 ± 226.0	
^{180}Ta$^{m}(n,\gamma)^{181}$Ta	30	1461.0 ± 122.0	1465.0 ± 100.0
	215	565.0 ± 48.0	
^{180}Ta$^{gs}(n,\gamma)^{181}$Ta	30	1495.0 ± 127.0	
	215	458.0 ± 46.0	
^{181}Ta$(n,\gamma)^{182}$Ta	30	857.0 ± 64.0	766.0 ± 15.0
	215	258.0 ± 23.0	

[a] Only theoretical estimate available.

$$N_A\langle\sigma v\rangle^*_{n,\gamma}(T) = \left(\frac{8}{\pi m}\right)^{1/2}\frac{N_A}{(kT)^{3/2}G(T)}\times \int_0^\infty \sum_\mu \frac{(2J^\mu_I+1)}{(2J^0_I+1)}\sigma^\mu_{n,\gamma}(E_n)E_n\exp\left(-\frac{E_n+E^\mu_x}{kT}\right)dE, \quad (2)$$

where N_A is the Avogadro's number and k is the Boltzmann constant. The temperature-dependent normalized partition function $G(T)=\sum_\mu(2J^\mu_I+1)/(2J^0_I+1)\exp(-E^\mu_x/kT)$ can completely specify the state distribution of the target. When $\mu=0$, Eq. (2) gives the reaction rate for the target in its ground state (*i.e.* laboratory reaction rates). The thermonuclear reaction rates were computed for the astrophysical temperatures T_9 in GK ($T_9 \equiv T/10^9$ K) ranging from $0.0001 \le T_9 \le 10$. For targets in thermal equilibrium, where the principle of detailed balance is valid [28], the reverse photo-neutron emission rates ^{180,181,182}Ta(γ,n) are also obtained. The astrophysical MACS $\langle\sigma v\rangle_{n,\gamma}/v_T$, where v_T is the relative thermal velocity $v_T=\sqrt{2kT/m}$, were calculated for each data set of all the ^{179,180,181}Ta(n,γ) reactions, at the *s*- and *p*-process thermal energies of $kT=30$ keV and $kT=215$ keV, respectively. The MACS were calculated for each $\sigma^\mu_{n,\gamma}(E_n)$ obtained from the individually measured NLDs and γSFs. The individual MACS for each of the (n,γ) reactions ^{179,180,181}Ta(n,γ) were combined through the weighted averages and are shown in Table 1, together with the available KADoNiS (v0.3) MACS [41] at *s*-process temperatures.

4. Nucleosynthesis application

Here, it is not the intention to give a complete review of the ^{180}Ta nucleosynthesis in different astrophysical sites, but rather to re-estimate, in light of the newly determined ^{179}Ta$(n,\gamma)^{180}$Ta^{gs,m}, ^{180}Ta$^{gs,m}(n,\gamma)^{181}$Ta and ^{181}Ta$(n,\gamma)^{182}$Ta rates, the ^{180}Ta and ^{181}Ta yields originating from the *s*-process in Asymptotic Giant Branch (AGB) stars and the *p*-process in massive stars exploding as Type-II supernovae. Both processes are studied below.

4.1. S-process production of ^{180}Ta^{m} and ^{181}Ta

For the *s*-process production of ^{180}Ta^{m} and ^{181}Ta, we have performed stellar evolution calculations to follow the complex production of ^{180}Ta during the thermally pulsing AGB phase. AGB models have been computed with the STAREVOL code [42,43] using an extended *s*-process reaction network of 411 species and the same

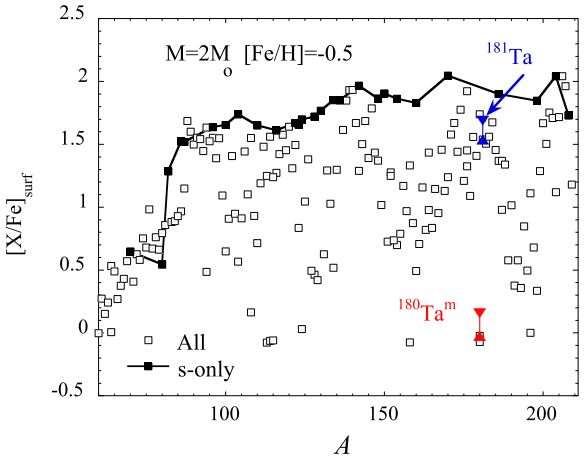

Fig. 2. Surface overabundances $[X/\mathrm{Fe}] = \log_{10}[X/X_\odot] - \log_{10}[\mathrm{Fe}/\mathrm{Fe}_\odot]$ as a function of the atomic mass A for all nuclei (dotted squares) or s-only nuclei (solid squares) at the end of the AGB phase, *i.e.* after the 29th thermal pulse, of the 2 $M_\odot$ [Fe/H] $= -0.5$ model star. Highlighted are the ^{180}Ta^m (red triangles) and ^{181}Ta (blue triangles) overabundances and their uncertainties associated with the reaction rates studied in the present work as well as those affecting the ^{179}Hf$(\beta^-)^{179}$Ta decay rate (see text for more details).

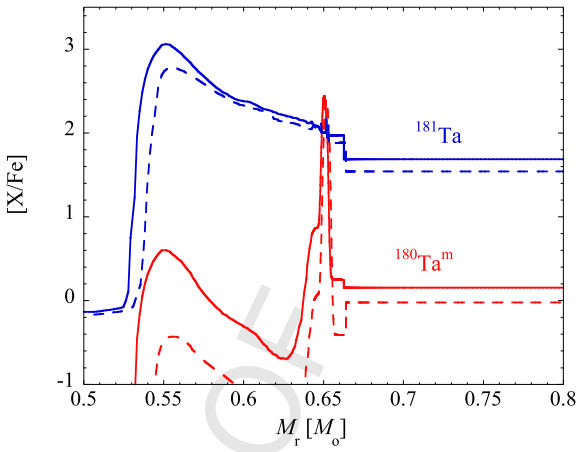

Fig. 3. Upper (solid line) and lower limits (dashed line) of the ^{180}Ta^m (red lines) and ^{181}Ta (blue lines) overabundances $[X/\mathrm{Fe}]$ inside the star, just below the convective envelope, as a function of the mass coordinate M_r after the 26th thermal pulse of our 2 $M_\odot$ [Fe/H] $= -0.5$ model star. The upper and lower limits are associated with the reaction rates uncertainties from the present work as well as those affecting the ^{179}Hf$(\beta^-)^{179}$Ta decay rate (see text for more details). The convective envelope extends above $M_r = 0.665$ $M_\odot$.

input physics as described in Ref. [44]. We focus here on a standard 2 $M_\odot$ [Fe/H] $= -0.5$ model star known to produce the main s-process elements ranging between $A = 90$ and $A = 204$. In the present calculation, a diffusion equation is used to simulate the partial mixing of protons in the C-rich layers at the time of the third dredge-up. Following the formalism of Eq. (9) of Ref. [44], the diffusive mixing parameters adopted in our calculations are $D_{min} = 10^9$ cm^2/s and $p = 5$, where D_{min} is the value of the diffusion coefficient at the innermost boundary of the convective envelope and p is an additional free parameter defining the slope of the exponential decrease of the overshoot diffusion coefficient with depth.

When not available experimentally, the cross sections were calculated within the statistical Hauser-Feshbach model with the TALYS reaction code [20,45]. The TALYS calculations were also used systematically to deduce from the laboratory neutron capture cross sections the stellar rates by allowing for the possible thermalization of low-lying states in the target nuclei. We note that at low temperature, the non-thermalization of the isomeric states of ^{26}Al, ^{85}Kr, ^{115}In, ^{176}Lu and ^{180}Ta is introduced explicitly in the reaction network [12,46]. Despite some studies predicting the thermalization of the ^{180}Ta ground and isomeric states at a temperature exceeding 25 keV [47,48], we assume here that both states are not thermalized at the temperatures found in our 2 $M_\odot$ [Fe/H] $= -0.5$ model star. The temperature- and density-dependent β-decay and electron capture rates in stellar conditions were taken from Ref. [49] with the update of Ref. [50]. Most importantly, the factor of about 3 for the uncertainties associated with the ^{179}Hf$(\beta^-)^{179}$Ta, as well as the 20–30% impact on the ^{179}Ta(EC)^{179}Hf decay rate are taken into account following the uncertain $\log ft$ transition rates considered in Ref. [50].

The ^{180}Ta nucleosynthesis by the s-process is known to be sensitive to the ^{179}Hf β-decay rate, the ^{179}Ta neutron capture cross sections and the potential depopulation by thermal photons of the isomeric state via intermediate states to the short-lived ground state. We analyze now the sensitivity of the ^{180}Ta production in our 2 $M_\odot$ [Fe/H] $= -0.5$ model star for the different nuclear and β-decay rates affecting directly the synthesis of ^{180,181}Ta. We show in Fig. 2 the resulting surface overabundances of elements heavier than Fe at the end of the AGB phase, *i.e.* after the 29th thermal pulse. While ^{181}Ta is relatively well produced with respect to the overall surface enrichment of s-only nuclei with an overabundance of about 1.7–2 dex, ^{180}Ta is seen to be strongly underabundant by a factor of about 100 in comparison with s-nuclei. As shown in Fig. 3, illustrating the profiles of ^{180}Ta^m and ^{181}Ta inside the star, ^{180}Ta^m is not present in the envelope ($M_r \gtrsim 0.67$ $M_\odot$), but its abundance peaks at about 2 dex in a thin layer below the convective envelope. This region lies just below the bottom of the thermal pulse where the temperature is high enough to favor a significant decay of ^{179}Hf into ^{179}Ta followed by a neutron capture, with the neutron stemming from the ^{22}Ne$(\alpha, n)^{25}$Mg reaction, hence a production of ^{180}Ta. Note that at a temperature 0.1 T_9, the ^{179}Hf$(\beta^-)^{179}$Ta decay timescale is about 2 Gyr while at 0.3 T_9, it falls to about 25 yr. However, the neutron captures take place below the thermal pulse where ^{22}Ne has been produced from the previous thermal pulse. Consequently this ^{180}Ta-rich region is not engulfed in the convective pulse, nor by the third dredge-up bringing the ashes of the interpulse and pulse nucleosynthesis up to the surface. Similar results concerning the absence of ^{180}Ta surface enrichment are found for AGB stars with an initial mass of 1.5 to 3.5 $M_\odot$. For this reason, contributions of low-mass AGB stars to the ^{180}Ta galactic enrichment can be expected to be relatively negligible.

4.2. *P-process production of* ^{180}Ta

Now we study the p-process nucleosynthesis on the basis of the Type-II supernova model, as described in [2,6,51], *i.e.* a model for a $Z_\odot$ 8 $M_\odot$ helium star (main sequence mass of about 25 $M_\odot$) evolved from the beginning of core He burning to the supernova explosion. We consider the 25 layers in the O/Ne-rich zone with explosion temperatures peaking between 1.7–3.3 T_9 responsible for the production of the p-elements. Their total mass is about 0.75 $M_\odot$. The deepest layer is located at a mass of about 1.94 $M_\odot$, which is far enough from the mass cut for all the nuclides produced in this region to be ejected during the explosion. All nucleosynthesis calculations have assumed here the absence of neutrinos.

Fig. 4 shows the overproduction factors $[X/X_\odot]$ resulting from the explosive nucleosynthesis in the 0.75 $M_\odot$ O/Ne-rich layers of the 25 $M_\odot$ star. The ^{180}Ta$(\gamma, n)^{179}$Ta destruction and ^{181}Ta$(\gamma, n)^{180}$Ta production rates (estimated from the detailed

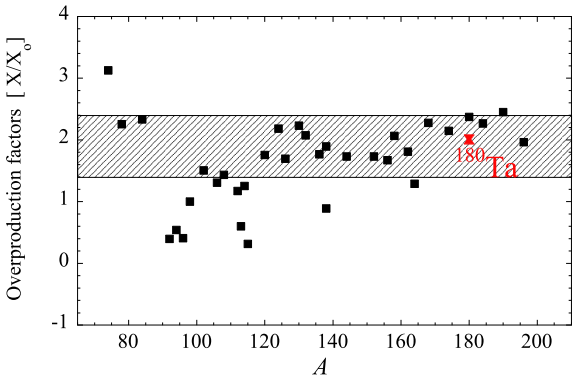

Fig. 4. P-nuclide overproduction factors $[X/X_{\odot}]$ obtained for the $Z = Z_{\odot}$ 25 $M_{\odot}$ model star with TALYS rates and the new Ta production and destruction rates. The ^{180}Ta value corresponds to the total ground state plus isomeric overabundances. The shaded region delineates a factor of 3 around a mean value. For more details see [2,3].

balance relation) and their associated uncertainties used in the present simulation correspond to the present experimentally constrained values (see Sect. 3). Only these rates are modified in the simulation and different combinations considered to estimate their impact on the nucleosynthesis. The resulting uncertainties are seen in Fig. 4 to give rise to a rather small error bar on the ^{180}Ta overproduction factor. As shown in Table 1, the new experimentally constraints essentially affect the ^{179}Ta(n,γ) MACS by increasing it by a factor of about 1.5 with respect to the only previously available theoretical estimates (KaDoNiS). Such an increase also impact the reverse ^{180}Ta(γ,n) destruction rate leading to a decrease of the ^{180}Ta^m by a factor 1.35 with respect to the yields that would have been obtained with the KaDoNiS rates.

The final ^{180}Ta overproduction is clearly compatible with the p-process enrichment of the other p-nuclei (even neglecting the neutrino effects). Two major effects may still affect the total abundance of ^{180}Ta given in Fig. 4. The first one concerns the possible increase of the ^{180}Ta production by neutrino captures [2,10]. For a total neutrino luminosity $L_{\nu} = 2.3 \times 10^{52}$ ergs s^{-1}, and neutrino temperatures of $T_{\nu_e} = 2.8$ MeV and $T_{\bar{\nu}_e} = T_{\nu_{\mu,\tau}} = 4.0$ MeV [10], we find that the ^{180}Ta abundance is increased by a factor of 1.3, and for a luminosity ten times larger, $L_{\nu} = 2.3 \times 10^{53}$ ergs s^{-1}, by a factor of 4. The charged current capture on ^{180}Hf is found to be the major contributor, while the neutral current on ^{181}Ta leads to a contribution twice smaller than the charged current one, as also found in Ref. [10]. Obviously, the impact of this extra production is still subject to all the uncertainties related to the neutrino physics, and in particular to the neutrino luminosity, temperature, oscillation and interaction cross sections. Note however that the recent measurement of the ^{180}Hf Gamow-Teller strength significantly constrain the ^{180}Hf(ν_e, e^-) rate [9].

A second effect arises from the freeze-out of the thermal equilibrium between the isomeric and ground states of ^{180}Ta at temperatures below $\simeq$ 0.3–0.4 T_9 [3,47,48]. The ^{180}Ta yields displayed in Fig. 4 are obtained under the assumption that ^{180}Ta remains equilibrated until the photoreactions responsible for its production and destruction freeze out. The abundance left over in the isomeric state critically depends on the temperature at which the ground and isomeric states stop thermalizing. For a critical temperature of 0.3–0.4 T_9, about 40% of the total ^{180}Ta abundance initially produced during the p-process ends up in the long-lived isomeric state, and consequently contributes to the galactic enrichment (for more details, see Ref. [3]). The conclusion that ^{180}Ta is essentially produced by the p-process is considered to be robust, and to hold irrespective of the intricacies and uncertainties related to the rates of the main photodisintegrations responsible for its production and destruction, to the thermal equilibration of ^{180}Ta, or to the details of the SNII models, at least in their spherically symmetric one-dimensional approximation.

5. Summary

In summary, the ^{180,181,182}Ta NLDs and γSFs obtained experimentally [14] are used as input parameters in the TALYS reaction code to calculate the ^{179,180,181}Ta radiative (n,γ) cross sections. From these, the Maxwellian averaged (n,γ) cross sections (MACS) and reaction rates of astrophysical interest are obtained. The compatibility of the new measurements with other experimental data supports the approach to use statistical properties i.e. NLDs and γSFs to estimate radiative capture cross sections, MACS and reaction rates. The latter are used in s-process calculations in AGB stars and p-process simulations in Type-II supernovae to investigate the nucleosynthesis of ^{180}Ta. The newly constrained reaction rates from this work show that the s-process contribution in low-mass AGB stars to the production of ^{180}Ta galactic enrichment is negligible and that ^{181}Ta is partially produced by AGB stars. The p-process nucleosynthesis of nature's rarest stable isotope ^{180}Ta in Type-II supernovae using new constraints from the current experimental measurements is significant and therefore suggests the p-process to be the fundamental production mechanism of ^{180}Ta^m in the universe. Detailed calculations in additional models stars both for AGBs and SN progenitors will further help in understanding the overall ^{180}Ta enrichment of the galaxy.

Acknowledgements

This work was supported by the National Research Foundation of South Africa under grant Nos. 100465, 92600, and 92789, by the IAEA under Research Contract 20454, the U.S. Department of Energy under contract No. DE-AC52-07NA27344. A.C.L. gratefully acknowledges support from the ERC-STG-2014 under grant agreement No. 637686 and the authors gratefully acknowledge funding from the Research Council of Norway, project grant No. 222287 (G.M.T.) and project grant No. 263030 (A.G., V.W.I., S.S., and F.Z.). S.G. acknowledges the support of the F.R.S. - FNRS.

References

[1] T. Rauscher, N. Dauphas, I. Dillmann, C. Fröhlich, Z. Fülöp, G. Gyürky, Constraining the astrophysical origin of the p-nuclei through nuclear physics and meteoritic data, Rep. Prog. Phys. 76 (2013) 066201.
[2] S. Goriely, M. Arnould, I. Borzov, M. Rayet, The puzzle of the synthesis of the rare nuclide ^{138}La, Astron. Astrophys. 375 (2001) L35–L38.
[3] M. Arnould, S. Goriely, The p-process of stellar nucleosynthesis: astrophysics and nuclear physics status, Phys. Rep. 384 (2003) 1–84.
[4] B.V. Kheswa, M. Wiedeking, F. Giacoppo, S. Goriely, M. Guttormsen, A. Larsen, F.L.B. Garrote, T. Eriksen, A. Görgen, T. Hagen, P. Koehler, M. Klintefjord, H. Nyhus, P. Papka, T. Renstrøm, S. Rose, E. Sahin, S. Siem, T. Tornyi, Galactic production of ^{138}La: impact of ^{138,139}La statistical properties, Phys. Lett. B 744 (2015) 268–272.
[5] A. Heger, E. Kolbe, W. Haxton, K. Langanke, G. Martínez-Pinedo, S. Woosley, Neutrino nucleosynthesis, Phys. Lett. B 606 (2005) 258.
[6] M. Rayet, M. Hashimoto, N. Prantzos, K. Nomoto, The p-process in type II supernovae, Astron. Astrophys. 298 (1995) 517.
[7] H. Utsunomiya, H. Akimune, S. Goko, M. Ohta, H. Ueda, T. Yamagata, K. Yamasaki, H. Ohgaki, H. Toyokawa, Y.-W. Lui, T. Hayakawa, T. Shizuma, E. Khan, S. Goriely, Cross section measurements of the ^{181}Ta$(\gamma,n)^{180}$Ta reaction near neutron threshold and the p-process nucleosynthesis, Phys. Rev. C 67 (2003) 015807.
[8] S.E. Woosley, D.H. Hartmann, R.D. Hoffman, W.C. Haxton, The ν-process, Astrophys. J. 356 (1990) 272.
[9] A. Byelikov, T. Adachi, H. Fujita, K. Fujita, Y. Fujita, K. Hatanaka, A. Heger, Y. Kalmykov, K. Kawase, K. Langanke, G. Martínez-Pinedo, K. Nakanishi, P. von Neumann-Cosel, R. Neveling, A. Richter, N. Sakamoto, Y. Sakemi, A. Shevchenko, Y. Shimbara, Y. Shimizu, F.D. Smit, Y. Tameshige, A. Tamii, S.E. Woosley, M.

Yosoi, Gamow-Teller strength in the exotic odd-odd nuclei ^{138}La and ^{180}Ta and its relevance for neutrino nucleosynthesis, Phys. Rev. Lett. 98 (2007) 082501.
[10] A. Sieverding, G. Martínez-Pinedo, L. Huther, K. Langanke, A. Heger, The ν-process in the light of an improved understanding of supernova neutrino spectra, Astrophys. J. 865 (2018) 143.
[11] H. Beer, R.A. Ward, Neutron-capture nucleosynthesis of nature's rarest stable isotope, Nature 291 (1981) 308–310.
[12] F. Käppeler, H. Beer, K. Wisshak, s-process nucleosynthesis-nuclear physics and the classical model, Rep. Prog. Phys. 52 (1989) 945–1013.
[13] S. Bisterzo, R. Gallino, F. Käppeler, M. Wiescher, G. Imbriani, O. Straniero, S. Cristallo, J. Görres, R.J. deBoer, The branchings of the main s-process: their sensitivity to α-induced reactions on ^{13}C and ^{13}Ne and to the uncertainties of the nuclear network, Mon. Not. R. Astron. Soc. 449 (2015) 506–527.
[14] C.P. Brits, K.L. Malatji, M. Wiedeking, B.V. Kheswa, S. Goriely, F.L.B. Garrote, D.L. Bleuel, F. Giacoppo, A. Görgen, M. Guttormsen, K. Hadynska-Klek, T.W. Hagen, S. Hilaire, V.W. Ingeberg, H. Jui, M. Klintefjord, A.C. Larsen, S.N.T. Majola, P. Papka, S. Péru, B. Qi, T. Renstrøm, S.J. Rose, E. Sahin, S. Siem, G.M. Tveten, F. Zeiser, Nuclear level densities and gamma-ray strength functions of ^{180,181,182}Ta, ArXiv e-prints, arXiv:1901.02682 [nucl-ex].
[15] K.L. Malatji, B.V. Kheswa, M. Wiedeking, F.L.B. Garrote, C.P. Brits, D.L. Bleuel, F. Giacoppo, A. Görgen, M. Guttormsen, K. Hadynska-Klek, T.W. Hagen, V.W. Ingeberg, M. Klintefjord, A.C. Larsen, H.T. Nyhus, T. Renstrøm, S. Rose, E. Sahin, S. Siem, G.M. Tveten, F. Zeiser, Nuclear level densities and γ-ray strength functions of ^{180,181}Ta and neutron capture cross sections, EPJ Web Conf. 146 (2017) 01010.
[16] T. Ericson, A statistical analysis of excited nuclear states, Nucl. Phys. 11 (1959) 481–491.
[17] M. Guttormsen, M. Aiche, F.L. Bello Garrote, L.A. Bernstein, D.L. Bleuel, Y. Byun, Q. Ducasse, T.K. Eriksen, F. Giacoppo, A. Görgen, F. Gunsing, T.W. Hagen, B. Jurado, M. Klintefjord, A.C. Larsen, L. Lebois, B. Leniau, H.T. Nyhus, T. Renstrøm, S.J. Rose, E. Sahin, S. Siem, T.G. Tornyi, G.M. Tveten, A. Voinov, M. Wiedeking, J. Wilson, Eur. Phys. J. A 51 (2015) 170.
[18] G.A. Bartholomew, E.D. Earle, A.J. Ferguson, J.W. Knowles, M.A. Lone, in: Advances in Nuclear Physics, vol. 7, Springer, 1973, pp. 229–317, Ch. 4.
[19] W. Hauser, H. Feshbach, The inelastic scattering of neutrons, Phys. Rev. 87 (1952) 366–373.
[20] A. Koning, D. Rochman, Modern nuclear data evaluation with the TALYS code system, Nucl. Data Sheets 113 (2012) 2841–2934.
[21] M. Guttormsen, A. Bürger, T. Hansen, N. Lietaer, The SiRi particle-telescope system, Nucl. Instrum. Methods Phys. Res., Sect. A 648 (2011) 168–173.
[22] M. Guttormsen, T. Tveter, L. Bergholt, F. Ingebretsen, J. Rekstad, The unfolding of continuum γ-ray spectra, Nucl. Instrum. Methods Phys. Res., Sect. A 374 (1996) 371–376.
[23] A. Schiller, L. Bergholt, M. Guttormsen, E. Melby, J. Rekstad, S. Siem, Extraction of level density and γ strength function from primary γ spectra, Nucl. Instrum. Methods Phys. Res., Sect. A 447 (2000) 498–511.
[24] M. Guttormsen, T. Ramsoey, J. Rekstad, The first generation of γ-rays from hot nuclei, Nucl. Instrum. Methods Phys. Res., Sect. A 255 (1987) 518–523.
[25] A.C. Larsen, M. Guttormsen, M. Krtička, E. Běták, A. Bürger, A. Görgen, H.T. Nyhus, J. Rekstad, A. Schiller, S. Siem, H.K. Toft, G.M. Tveten, A.V. Voinov, K. Wikan, Analysis of possible systematic errors in the Oslo method, Phys. Rev. C 83 (2011) 034315.
[26] A. Gilbert, A.G.W. Cameron, A composite nuclear-level density formula with shell corrections, Can. J. Phys. 43 (1965) 1446–1496.
[27] S. Goriely, S. Hilaire, A.J. Koning, Improved microscopic nuclear level densities within the Hartree-Fock-Bogoliubov plus combinatorial method, Phys. Rev. C 78 (2008) 064307.
[28] J. Holmes, S. Woosley, W.A. Fowler, B. Zimmerman, Tables of thermonuclear-reaction-rate data for neutron induced-reactions on heavy nuclei, At. Data Nucl. Data Tables 18 (1976) 305–412.
[29] A. Koning, J. Delaroche, Local and global nucleon optical models from 1 keV to 200 MeV, Nucl. Phys. A 713 (2003) 231–310.
[30] H. Hofmann, J. Richert, J. Tepel, H. Weidenmüller, Direct reactions and Hauser-Feshbach theory, Ann. Phys. 90 (1975) 403–437.
[31] V. Kononov, B. Jurlov, D. Poletaev, V. Timokhov, Sov. J. Nucl. Phys. 26 (1977) 500.
[32] M.V. Bokhovko, V.N. Kononov, E.D. Poletaev, N.S. Rabotnov, V.M. Timokhov, Average fast neutron radiative capture cross sections for fission products and for isotopes of rare earth elements, in: Nucl. Data Sci. Technology, Springer, Berlin, Heidelberg, 1992, pp. 62–64.
[33] M. Lindner, R.J. Nagle, J.H. Landrum, Neutron capture cross sections from 0.1 to 3 MeV by activation measurements, Nucl. Sci. Eng. 59 (1976) 381–394.
[34] K. Wisshak, F. Voss, C. Arlandini, F. Käppeler, M. Heil, R. Reifarth, M. Krtička, F. Bečvář, Stellar neutron capture on ^{180}Ta^m I. cross section measurement between 10 keV and 100 keV, Phys. Rev. C 69 (2004) 055801.
[35] S. Goko, H. Utsunomiya, S. Goriely, A. Makinaga, T. Kaihori, S. Hohara, H. Akimune, T. Yamagata, Y.W. Lui, H. Toyokawa, A.J. Koning, S. Hilaire, Partial photoneutron cross sections for the isomeric state ^{180}Ta^m, Phys. Rev. Lett. 96 (2006) 192501.
[36] M. Guttormsen, S. Goriely, A.C. Larsen, A. Görgen, T.W. Hagen, T. Renstrøm, S. Siem, N.U.H. Syed, G. Tagliente, H.K. Toft, H. Utsunomiya, A.V. Voinov, K. Wikan, Quasicontinuum γ decay of ^{91,92}Zr: benchmarking indirect (n,γ) cross section measurements for the s process, Phys. Rev. C 96 (2017) 024313.
[37] B.V. Kheswa, M. Wiedeking, J.A. Brown, A.C. Larsen, S. Goriely, M. Guttormsen, F.L.B. Garrote, L.A. Bernstein, D.L. Bleuel, T.K. Eriksen, F. Giacoppo, A. Görgen, B.L. Goldblum, T.W. Hagen, P.E. Koehler, M. Klintefjord, K.L. Malatji, J.E. Midtbø, H.T. Nyhus, P. Papka, T. Renstrøm, S.J. Rose, E. Sahin, S. Siem, T.G. Tornyi, Phys. Rev. C 95 (2017) 045805.
[38] A.C. Larsen, M. Guttormsen, R. Schwengner, D.L. Bleuel, S. Goriely, S. Harissopulos, F.L.B. Garrote, Y. Byun, T.K. Eriksen, F. Giacoppo, A. Görgen, T.W. Hagen, M. Klintefjord, T. Renstrøm, S.J. Rose, E. Sahin, S. Siem, T.G. Tornyi, G.M. Tveten, A.V. Voinov, M. Wiedeking, Experimentally constrained $(p,\gamma)^{89}$Y and $(n,\gamma)^{89}$Y reaction rates relevant top-process nucleosynthesis, Phys. Rev. C 93 (2016) 045810.
[39] A. Spyrou, S.N. Liddick, A.C. Larsen, M. Guttormsen, K. Cooper, A.C. Dombos, D.J. Morrissey, F. Naqvi, G. Perdikakis, S.J. Quinn, T. Renstrøm, J.A. Rodriguez, A. Simon, C.S. Sumithrarachchi, R.G.T. Zegers, Novel technique for constraining r-process (n,γ) reaction rates, Phys. Rev. Lett. 113 (2014) 232502.
[40] T. Renstrøm, H.T. Nyhus, H. Utsunomiya, R. Schwengner, S. Goriely, A.C. Larsen, D.M. Filipescu, I. Gheorghe, L.A. Bernstein, D.L. Bleuel, T. Glodariu, A. Görgen, M. Guttormsen, T.W. Hagen, B.V. Kheswa, Y.W. Lui, D. Negi, I.E. Ruud, T. Shima, S. Siem, K. Takahisa, O. Tesileanu, T.G. Tornyi, G.M. Tveten, M. Wiedeking, Low-energy enhancement in the γ-ray strength functions of ^{73,74}Ge, Phys. Rev. C 93 (2016) 064302.
[41] I. Dillmann, T. Szücs, R. Plag, Z. Fülöp, F. Käppeler, A. Mengoni, T. Rauscher, The Karlsruhe astrophysical database of nucleosynthesis in stars project - status and prospects, Nucl. Data Sheets 120 (2006) 171–174.
[42] L. Siess, E. Dufour, M. Forestini, An Internet server for update pre-main sequence tracks of low- and intermediate-mass stars, Astron. Astrophys. 358 (2000) 593–599.
[43] L. Siess, Evolution of massive AGB stars, Astron. Astrophys. 448 (2006) 717–729.
[44] S. Goriely, L. Siess, Sensitivity of the s-process nucleosynthesis in AGB stars to the overshoot model, Astron. Astrophys. 609 (2018) A29.
[45] S. Goriely, S. Hilaire, A.J. Koning, Improved predictions of nuclear reaction rates with the TALYS reaction code for astrophysical applications, Astron. Astrophys. 487 (2008) 767–774.
[46] Z. Nemeth, F. Käppeler, C. Theis, T. Belgya, S.W. Yates, Nucleosynthesis in the Cd-In-Sn region, Astrophys. J. 426 (1994) 357.
[47] D. Belic, C. Arlandini, J. Besserer, J. de Boer, J.J. Carroll, J. Enders, T. Hartmann, F. Käppeler, H. Kaiser, U. Kneissl, M. Loewe, H.J. Maier, H. Maser, P. Mohr, P. von Neumann-Cosel, A. Nord, H.H. Pitz, A. Richter, M. Schumann, S. Volz, A. Zilges, Photoactivation of ^{180}Ta^m and its implications for the nucleosynthesis of nature's rarest naturally occurring isotope, Phys. Rev. Lett. 83 (1999) 5242–5245.
[48] P. Mohr, F. Käppeler, R. Gallino, Survival of nature's rarest isotope ^{180}Ta under stellar conditions, Phys. Rev. C 75 (2007) 012802.
[49] K. Takahashi, K. Yokoi, Beta-decay rates of highly ionized heavy atoms in stellar interiors, At. Data Nucl. Data Tables 36 (1987) 375–409.
[50] S. Goriely, Uncertainties in the solar system r-abundance distribution, Astron. Astrophys. 342 (1999) 881–891.
[51] M. Hashimoto, Supernova nucleosynthesis in massive stars, Prog. Theor. Phys. 94 (1995) 663–736.

Please cite this article in press as: K.L. Malatji et al., Re-estimation of ^{180}Ta nucleosynthesis in light of newly constrained reaction rates, Phys. Lett. B (2019), https://doi.org/10.1016/j.physletb.2019.03.013